ELSEVIER

Journal of Structural Geology 28 (2006) 1244–1260

JOURNAL OF STRUCTURAL GEOLOGY

www.elsevier.com/locate/jsg

Neotectonic evolution and fault geometry change along a major extensional fault system in the Mission and Flathead Valleys, NW-Montana

Michael H. Hofmann *, Marc S. Hendrix, Michael Sperazza, Johnnie N. Moore

Department of Geology, University of Montana, Missoula, MT 59801, USA

Received 14 July 2005; received in revised form 10 March 2006; accepted 23 March 2006

Abstract

Analysis of 3.5 kHz high-resolution seismic data from Flathead Lake, combined with results from onshore geologic mapping and literature review from previous studies in the area, reveals a significant change in fault geometry and seismic activity along strike of the Mission Fault system in the Mission and Flathead Valleys of northwestern Montana. The Mission Fault system is composed of faults with normal sense of motion and faults with minor oblique-slip and strike-slip motion. It evolves from a single fault strand in the Mission Valley south of Flathead Lake into a multiple strand fault system in the Flathead Lake basin and north of the lake. Fault activity decreases to the north as suggested by northward decreasing fault scarp heights in the lake basin. North of the lake the Mission Fault system is truncated by oblique strike-slip faults and the extensional strain is accommodated by the Swan Fault, another major normal fault north and east of the study area. We observed five phases of increased tectonic activity in the lake basin during the last 15,000 years. The oldest phase (phase B), active between 15,000 and 13,000 cal yr BP, resulted in fault scarps with up to 14 m of relief along the Mission Fault and the Kalispell–Finley Point Fault. We calculated average displacement rates as high as 1 mm/yr for this oldest phase. Phases C–F represent smaller tectonic events in the lake basin during the last 10,000 cal yr BP. Offset of seismic reflectors during these younger events is generally at dm-scale, indicating relatively low average displacement rates.

Keywords: Neotectonic; 3.5 kHz High-resolution seismic data; NW-Montana; Pleistocene; Holocene; Extensional faulting

1. Introduction

The northern Basin and Range Province has emerged recently as an excellent natural laboratory to understand upper crustal deformational kinematics in a continental interior tectonic setting, in part because of the wide variety of deformational environments that occur there. These include fundamental structural lineaments such as the Lewis and Clark Line (e.g. Sears and Hendrix, 2004), metamorphic core complexes (e.g. O'Neill et al., 2004), and a variety of presumably shallower but seismically active extensional structures (e.g. Haller et al., 2000; Stickney et al., 2000; Fig. 1).

Most neotectonic studies in the northern Basin and Range Province, to this date, have been conducted in the southern part of this structural province, close to the epicenters of major historic earthquakes such as those at Hebgen Lake, Montana in 1959 and Borah Peak, Idaho in 1983 (Stickney and Bartholomew, 1987; Stickney, 1999; Haller et al., 2000; Pierce et al., 2000; Schwartz et al., 2000). Published neotectonic studies north of the Lewis and Clark Line in the Mission and Flathead Valleys of northwestern Montana have focused on land-based expressions of faults and their associated sediments (Fig. 1A; Stickney, 1980; Qamar et al., 1982; Harrison et al., 1986; Ostenaa et al., 1990, 1995; Lageson and Stickney, 2000). No published studies to date have used shallow seismic reflection data to interpret the neotectonic history in this area.

Flathead Lake (Fig. 1B) is a large, open lake basin with a surface area of approximately 496 km^2, located north of the Lewis and Clark Line in northwestern Montana. The lake provides an excellent opportunity to document the detailed geometry of Late Pleistocene and Holocene neotectonic features in this region because it is bounded on its eastern side by the Mission Fault, a major seismically active down-to-the-west normal fault. Additionally, the lake contains about 160 m of syn- and post-glacial deposits that appear to have captured the late Pleistocene and Holocene geologic and tectonic history of the region in great detail.

In this paper, we outline the neotectonic history of this region by combining results from onshore geologic mapping

* Corresponding author. Tel.: +1 406 243 5822; fax: +1 406 243 4028.
E-mail address: michael.hofmann@umontana.edu (M.H. Hofmann).

0191-8141/$ - see front matter © 2006 Elsevier Ltd. All rights reserved.
doi:10.1016/j.jsg.2006.03.030

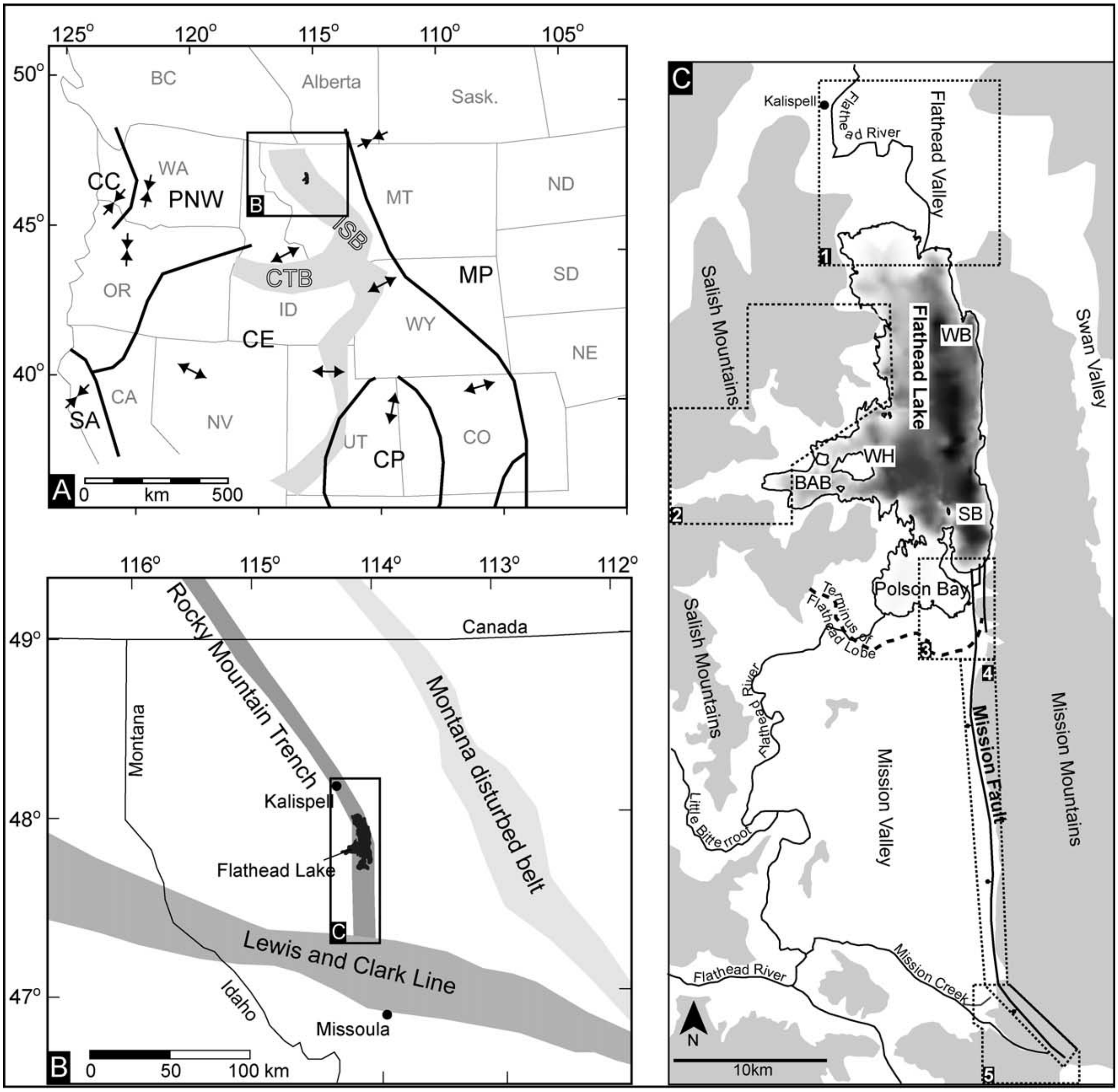

Fig. 1. (A) Generalized map of the western United States tectonic stress field and the location of relevant seismically active zones. Outward pointing arrows characterize areas of extensional stress; inward pointing arrows show areas with compressional tectonism. Stress provinces are separated by thick lines. ISB = Intermountain Seismic Belt; CTB = Centennial Tectonic Belt; CC = Cascade Convergent Province; PNW = Pacific Northwest; CE = Cordillera Extension; SA = San Andreas Province; CP = Colorado Plateau Interior; MP = Mid-Plate. (Stress field map adapted from Zoback and Zoback (1989).) (B) Map showing important regional structural features proximal to the study area. The Montana disturbed belt is an inactive compressional structural province. In contrast the Rocky Mountain Trench and the Lewis and Clark Line are tectonically active areas. (C) Map of the study area indicating areas of previous studies discussed in this paper (1 = Stickney (1980); 2 = LaPoint (1971) and Harrison et al. (1986); 3 = Hofmann and Hendrix (2004a); 4 = Ostenaa et al. (1995); 5 = Hofmann and Hendrix (2004b)). Bedrock outcrops are shaded in gray; white areas denote Quaternary sediments. Different shades of gray in the Flathead Lake basin represent the lake bathymetry with black being deeper than 100 m and white being less than 10 m deep. Also marked on this map is the trace of the Mission Fault south of the lake. BAB = Big Arm Bay; SB = Skidoo Bay; WB = Woods Bay; WH = Wild Horse Island.

with analysis of offshore high-resolution seismic reflection data from Flathead Lake. In addition, we use results from limited previous work in the area that focused mainly on movements along major faults around Flathead Lake and the locations of earthquakes along these faults (Smith and Sbar, 1974; Stickney, 1980, 1999; Qamar et al., 1982; Ostenaa et al., 1990; Haller et al., 2000; Lageson and Stickney, 2000; Stickney et al., 2000).

Understanding the neotectonic history of the Mission Fault system and discerning whether it and other major faults in the region are still active is important because of the potential seismic risks to fast growing communities in western Montana, including those in Flathead and Missoula counties (combined 2000 census population of 170,000) and the history of major seismic ruptures in the area (e.g. Hebgen Lake). As reported by Ostenaa et al. (1995) and

Hofmann and Hendrix (2004a,b), current understanding of seismic risk in the region is inhibited by a lack of dateable material in local Quaternary glacial deposits that are deformed by extensional structures. This paper includes improvements in chronology made possible by tying deformed strata imaged in our seismic reflection data to several well-dated sediment cores from Flathead Lake (Hofmann et al., 2006). Herein, we focus on using this chronologically constrained seismic stratigraphic framework for Flathead Lake to refine the timing of deformational events expressed in its sediments and to interpret the geometry of the observed structures.

1.1. Structural setting

The study area is located at the intersection of two major structural provinces of western North America: the Rocky Mountain Trench and the Lewis and Clark Line (Fig. 1B). The Rocky Mountain Trench is a linear roughly north–south-trending trough, bounded on one, and sometimes both sides, by major normal faults. It is a linear system of valleys that extends for approximately 1600 km from northern Montana to the British Columbia–Yukon border (Leech, 1966). Although more recently published work seems to suggest that the Rocky Mountain Trench might not continue into the Mission Valley (Constenius, 1996), for convenience we will use the term Rocky Mountain Trench as described by Leech (1966) for the reminder of this study. In contrast, the Lewis and Clark Line trends ESE–WNW and is characterized by predominantly dextral strike-slip movement related to large magnitude clockwise rotation of crust during the Sevier Orogeny (Sears and Hendrix, 2004).

The study area is located in the northwestern extension of the Intermountain Seismic Belt (ISB) and has a rich history of active seismicity, as well as a significant prehistoric record of seismicity (Stickney et al., 2000). The ISB defines a belt of high seismicity that extends from the Flathead Lake Region south through western Montana, eastern Idaho, northwestern Wyoming, central Utah, and northernmost Arizona (Fig. 1A). Historic seismicity in the ISB typically is diffuse but is punctuated by the occurrence of magnitude 6.5–7.5 earthquakes, like the magnitude 7.5 Hebgen Lake earthquake of 1959, the largest historic earthquake that occurred within the ISB in Montana (Stickney et al., 2000).

Pleistocene and Holocene faults in the ISB typically are range-bounding normal faults that display evidence of recurrent, discrete, surface displacements of up to several meters during individual seismic events. Within the study area, geomorphically well-expressed fault scarps have been documented as offsetting Pleistocene and Holocene sediments. The last major event to have produced a surface rupture along the east side of the Mission Valley occurred 7700 ± 200 years ago with an estimated seismic moment of magnitude 7.5 (Ostenaa et al., 1995).

Many of the Quaternary extensional faults in the northern Basin and Range Province reactivate traces of older, mainly Mesozoic compressional faults (Constenius, 1996). The Rocky Mountain trench for example follows in depth an old basement ramp that is part of a Mesoproterozoic margin upon which the Belt Supergroup was deposited. During Mesozoic contraction, the Rocky Mountain Basal Detachment (RMBD) closely followed the craton-cover contact across this ramp, forming a major culmination above it (Sears, 2001). When thrusting ceased at the end of the Cretaceous, the RMBD and many smaller surficial thrust faults were reactivated as extensional faults during the early Paleocene (e.g. Constenius, 1996).

1.2. Stratigraphy

The sedimentary basement in the Mission and Flathead Valleys consists of metasedimentary rocks of the Mesoproterozoic Belt Supergroup that crop out widely in the mountain ranges along the margins of the study area and represent the deepest exposed stratigraphic level (Harrison et al., 1986; Fig. 1C). Paleogene strata in the study area may exist north of Flathead Lake in the Flathead Valley (Smith, 2004), but has not been identified within the Flathead Lake basin and in the Mission Valley immediately south of the lake (Hofmann et al., 2006).

Pleistocene sediments associated with the last glacial maximum are most widespread in the study area, because it is located at the former terminal position of the Flathead Lobe of the Cordilleran Ice Sheet (Fig. 1C). Related sediments include ice-contact deposits, widespread glacio-fluvial deposits, local eolian deposits, and glaciolacustrine deposits associated with glacial Lake Missoula (Pardee, 1910, 1942; Davis, 1920; Nobles, 1952; Alden, 1953; Ostenaa et al., 1995; Levish, 1997; Smith, 2004; Hofmann and Hendrix, 2004a). Locally overlying these Pleistocene sediments are Holocene fluvial, alluvial, and eolian deposits. Seismic reflection data suggest that Flathead Lake itself contains up to 160 m of sedimentary strata (Wold, 1982; Hofmann et al., 2006). In the upper part of this sedimentary succession, which is well imaged on the 3.5 kHz data set, lake deposits of late Pleistocene and Holocene age are preserved.

Hofmann et al. (2006) identified six different seismic stratigraphic units (A–F) and several unconformities in the Flathead Lake seismic data set (Fig. 2). Seismic stratigraphic unit A consists mainly of chaotic seismic reflections that likely are glacial till related to the last glacial occupation of the lake basin and presumably correlates to glacial till found in several moraines onshore (Smith, 1977; Hofmann and Hendrix, 2004a). Parallel high amplitude reflections of unit B are inferred to represent glacial rhythmites, deposited in a proglacial lake during retreat of the Cordilleran Ice Sheet. A ^{14}C date from the upper part of this unit suggests a depositional age older than 14,150 ± 150 cal yr BP (Hofmann et al., 2006). Unit C is a composite of several different seismic facies that include event deposits that post-date the glacial retreat (Hofmann et al., 2006). Seismic stratigraphic unit D reflects deposition in a lake with a stable lake level at a relative highstand. By approximately 7600 cal yr BP lake level had dropped an estimated 15 m below the present level, exposing

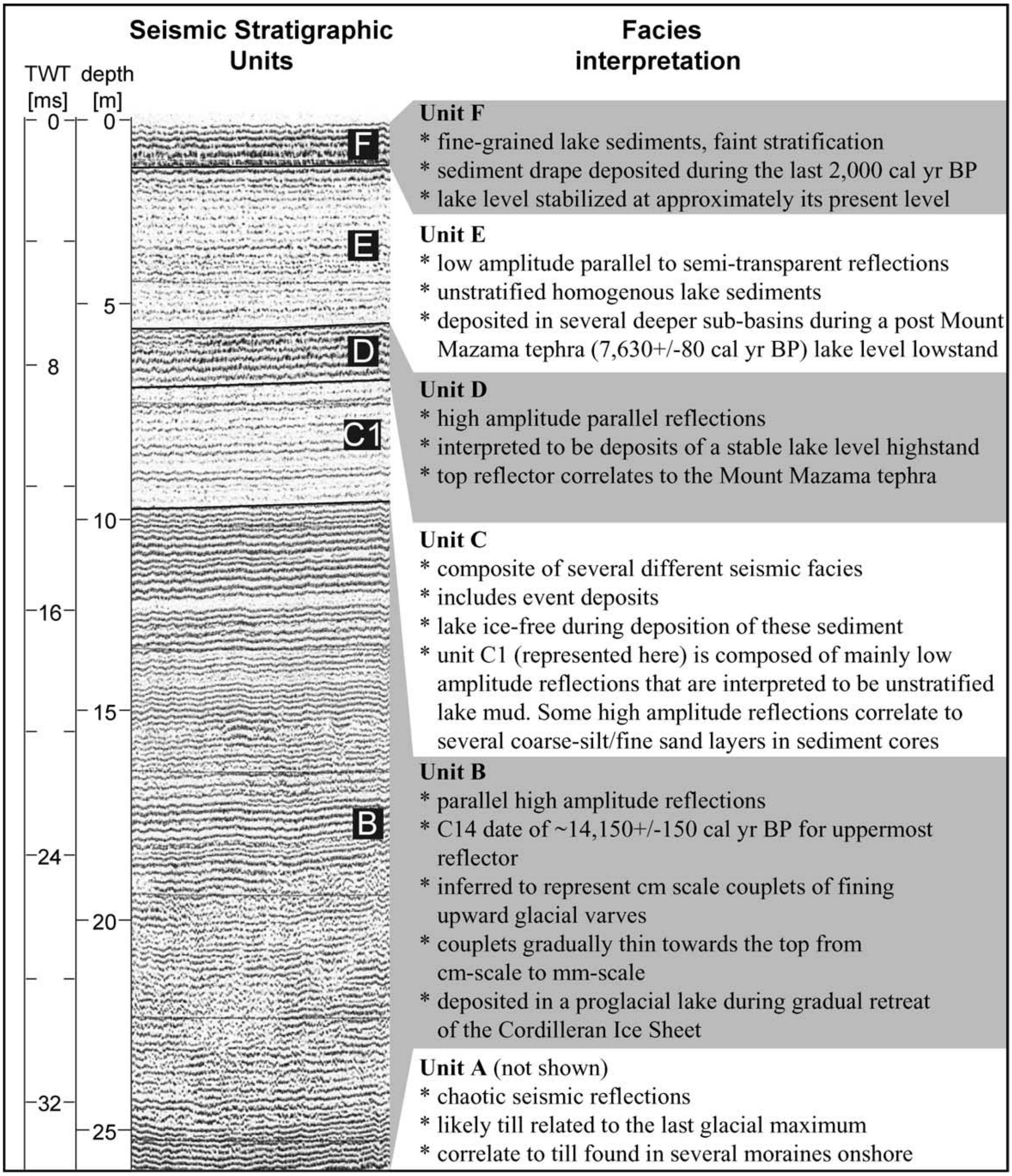

Fig. 2. Display of the different seismic stratigraphic units B–F and accompanying seismic facies interpretation (modified from Hofmann et al., 2006).

many shallow parts of Big Arm Bay and Polson Bay. As a result, seismic stratigraphic unit E was deposited only within some deeper, bathymetrically-closed basins in Big Arm Bay and in the deeper parts of the lake east of Wild Horse Island (Fig. 1C). However, onlap geometries of seismic reflections suggest a gradual lake level rise during deposition of seismic unit E. Finally, unit F represents a drape of lake sediments deposited during the last ~2000 cal yr BP, as the lake level stabilized approximately at its present elevation. Lake sediments associated with the pro-glacial lake stage and the higher Holocene lake stages are exposed locally onshore, but usually are difficult to correlate due to the lack of dateable ^{14}C material.

2. Data sets and methods

Our main data set consists of 270 km of high-resolution 3.5 kHz seismic data, originally collected and described by Kogan (1980) and more recently interpreted by Hofmann et al. (2006). Data acquisition and processing is described in more detail in these two previous studies and will not be discussed here. For depth conversion of the two-way-travel time data we followed the results of Hofmann et al. (2006) and assumed acoustic velocities of 1.45 m/ms in water and 1.5 m/ms for the shallowest sediments, consistent with experimental acoustic impedance studies in other lakes (Finckh et al., 1984; Mullins et al., 1996). These time–depth conversions result in useful imaging of the uppermost 60 m of sediments in Flathead Lake with a resolution of approximately 30–40 cm.

For our onshore analyses we used available geologic (Harrison et al., 1986; Hendrix et al., 2004; Hofmann and Hendrix, 2004a), structural (Harrison et al., 1986; Ostenaa et al., 1995), and topographic maps to identify onshore strands of the Mission Fault. In addition, we applied stream length-gradient index (SL) and mountain front sinuosity (S_{mf})

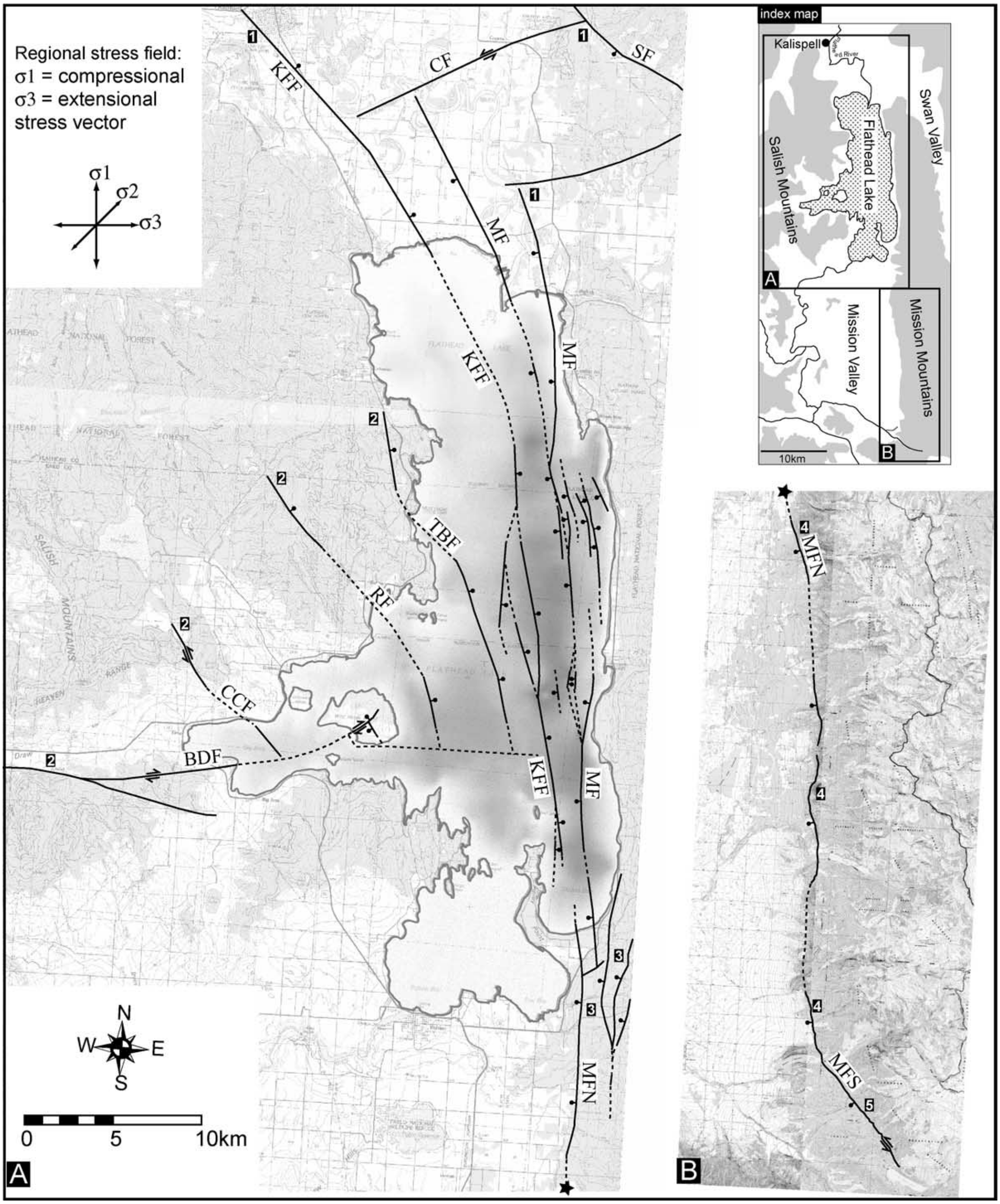

Fig. 3. Map showing the fault traces in the study area. Most faults are located in the eastern part of the lake basin and line up with the Mission Fault system. The main fault traces are the west dipping Mission Fault (MF) and the east dipping Kalispell–Finley Point Fault (KFF), both composed of several fault splays. Other main faults in the study area are the east dipping Table Bay Fault (TBF), the also east dipping Rollins Fault (RF), the left-lateral strike-slip Chief Cliff Fault (CCF), and the right-lateral strike-slip Big Draw Fault (BDF). North of the lake the Mission Fault is truncated by the left-lateral strike-slip Carson Fault (CF) and the extensional stress is accommodated by the Swan Fault (SF), another major north–south-trending normal fault located north and east of the study area. Note the change in structural style from a single surficial fault splay in the Mission Valley (map B) to multiple fault splays in the lake basin (map A). Small faults are not labeled on this map and some faults that do not strike north–south but rather strike at an angle and have inferred strike-slip motion are not displayed. Faults onshore have been adapted from (1) Stickney (1980); (2) LaPoint (1971) and Harrison et al. (1986); (3) Hofmann and Hendrix (2004a); (4) Ostenaa et al. (1995); and (5) Hofmann and Hendrix (2004b). MFN = Mission Fault North; MFS = Mission Fault South.

morphometric parameters (Keller and Pinter, 1996) to quantify tectonic activity indices and slip rates for the onshore segments of this fault system.

From these two morphometric parameters we were able to estimate tectonic activity rates of the fault segments and compare these activity rates with displacement rates as independent indices of fault activity. Mountain fronts in semi-arid regions, like the study area, are characteristic of the highest relative tectonic activity class of 1 and typically have high fault displacement rates in the range of 1.0–5.0 mm/yr (Rockwell et al., 1985; Bull, 1987). Such regions usually have very low values of S_{mf} (<1.1) and the highest SL indices in a particular region (Keller and Pinter, 1996). In contrast, the lowest tectonic activity class, class 5, is characterized by high S_{mf} values, generally in the range of 2.6–4.0, and relatively low SL indices (Rockwell et al., 1985).

2.1. Sources of error

Several different possible sources of error regarding data processing and interpretation must be considered in this study. Due to the originally analog nature of the seismic data set, it was necessary to scan the original seismic lines prior to analysis on a computer. During the scanning process, some of the data might have been slightly distorted. Tie-points for the seismic lines assigned in ArcGIS were mostly adapted from the line traces on the original maps produced during the seismic data acquisition process (Kogan, 1980). Errors in the original location of seismic lines, which were located with the use of compass and sextant, therefore would carry through to the present analysis. In addition, we assigned a 90 m grid to Flathead Lake to produce our digital maps, resulting in an additional accuracy uncertainty of 45 m for some of the data points. Although the use of modern GPS locating techniques obviously would reduce this uncertainty, analytic errors contained in the seismic data set do not affect the overall results of our study in terms of defining the broad geometry of fault segments within Flathead Lake or in terms of constraining the timing of seismic activity preserved in the sediment record.

Other possible sources of error in this study include (1) the possibility that faults were not adequately imaged on the seismic grid and so were not recognized, (2) uncertainties regarding the degree to which compaction of sediments affects sedimentation rate calculations, (3) combining chronologic and sedimentary thickness measurements to estimate displacement rates and timing of seismic events, and (4) a lack of seismic data from the southern part of the lake.

Inadequate coverage of the southern parts of Flathead Lake during the seismic survey might be the cause for an underestimation of fault activity in this part of the lake. The recognition of active faulting in sedimentary basins depends on the relative balance between fault slip rate and sedimentation rate. In areas with high sedimentation rates and slow fault slip, fault displacements may not be imaged in seismic profiles, hence the number and offset magnitude of faults may be underestimated. To assess whether compaction has to be addressed as a significant source of error we calculated porosity changes for different burial depths using standard compaction equations (e.g. Miall, 2000). Porosity in the lake sediments is decreased approximately 1% in 10 m burial depth and between 3.5 and 5% 60 m below the sediment water interface. Hence, thickness changes due to compaction within the upper 25 m of the sediment column are below seismic resolution and therefore negligible. Sedimentation rates for Flathead Lake were calculated from core data as being in a range of 0.4–0.6 mm/yr for seismic units C–F and significantly higher, up to approximately 20–80 mm/yr, for seismic unit B. These sedimentation rate calculations and the stated seismic resolution of 30–40 cm result in an average age estimation uncertainty of 500–1000 years for seismic units C–F and 4–20 years for seismic unit B. This uncertainty excludes error associated with ^{14}C dating or other chronologic methods employed in this study.

3. Results and discussion

3.1. Neotectonic structural framework

Reverse faults, thrust faults, strike-slip faults, and normal faults have all been observed in northwestern Montana. Most reverse and thrust faults are related to pre-Pleistocene orogenic events and are not the focus of this study. Active faults with normal and, to a lesser extent, strike-slip sense of motion mainly compensate extensional stress in the study area and are focused upon below. In the text that follows, we describe in detail the geometry of these two fault types and how they are distributed across the Mission and southern Flathead Valleys and in the Flathead Lake basin itself.

3.1.1. Onshore faults

Onshore surface traces of faults with normal and strike-slip components have been mapped and described in the area around Flathead Lake (Harrison et al., 1986; Ostenaa et al., 1995; Hendrix et al., 2004; Hofmann and Hendrix, 2004a,b). Some of these faults were reported active during the late

Fig. 4. Map of fault segments that were active during at least one of the tectonic activity phases (B–F) in the Flathead Lake basin. The tectonic phases are named after the youngest reflectors that are cut by a fault. Phase B (map A) is the oldest phase and includes fault segments that were active between 15,000 and 13,000 cal yr BP (fault segments B1–B7), hence cut reflections of seismic unit B. The main rupture event, tectonic phase B, is considered to be the largest magnitude seismic event in the lake basin. This oldest tectonic event also offset onshore exposed glacial sediments along the Mission Fault further to the south in the Mission Valley (see Fig. 3). Phases C–F are considered to be more local events and only offset seismic reflections at dm scale. Phase C (map B) includes seismic events that ruptured the area at ~10,000 cal yr BP (fault segments C1–C6), phase D (map C) at 7600–8000 cal yr BP (fault segments D1–D4), and phases E and F (map D) include minor seismic events that offset the prominent reflector of the Mount Mazama tephra (fault segments E1, E2 and F1).

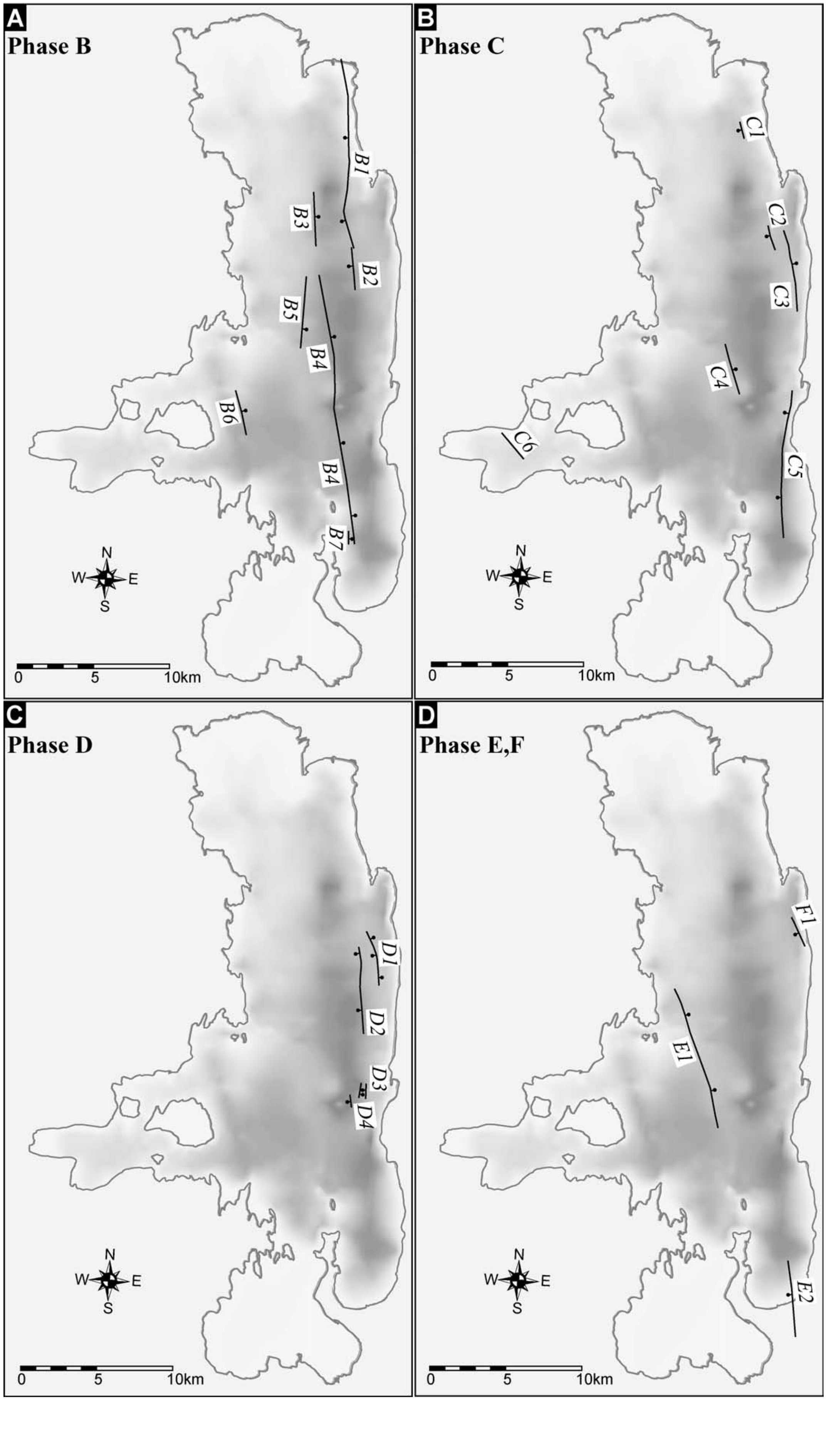
A
Phase B
B1
B2
B3
B4
B5
B6
B4
B7
B
Phase C
C1
C2
C3
C4
C5
C6
C
Phase D
D1
D2
D3
D4
D
Phase E,F
F1
E1
E2
N
W
E
S
0
5
10km

Pleistocene and Holocene while others do not show any obvious signs of late Pleistocene and Holocene offset. The most prominent of the active faults is the Mission Fault, a normal fault south and east of Flathead Lake (Figs. 1C and 3; Ostenaa et al., 1990, 1995). Below, we describe the geometry of this fault along three different fault segments.

The southernmost segment of the Mission Fault is 6.6 km long, strikes 135° and is located between St. Mary's Lake and Mission Reservoir (Fig. 3B; Hofmann and Hendrix, 2004b). Trenching studies by Ostenaa et al. (1995) suggested that the last surface-faulting event in this area occurred about 7700 ± 200 cal yr BP based on the observation that the Mount Mazama ash (7630 ± 80 cal yr BP; Zdanowicz, 1999) blankets ruptured sediments. The minimum fault displacement was approximately 2 m during this last rupture, but the scarps along this segment were reported to be more than 12 m high and thus likely a product of more than one faulting event (Ostenaa et al., 1995). The overall displacement for bedrock along this segment of the fault may be more than 5 km (Ostenaa et al., 1990), with a significant component of dextral slip superimposed on an otherwise mainly normal sense of movement (Witkind, 1975; Haller, 1995; Ostenaa et al., 1995). We calculated a mountain-front sinuosity (S_{mf}) of 1.3, and stream length-gradient (SL) index of 213–975 (mean = 584) for this segment of the Mission Fault.

In contrast to the Holocene tectonic activity reported along the southern segment, trenching studies and mapping along the northern segment of the Mission Fault in the vicinity of Flathead Lake show that the last rupture event in this area occurred shortly after the retreat of the Cordilleran Ice Sheet. The northern segment of the Mission Fault consists of numerous sub-parallel traces that offset till associated with the last glacial maximum (Fig. 3A; Haller, 1995; Hofmann and Hendrix, 2004a). Many of the fault splays do not appear to displace Quaternary deposits, and the timing of movement along these splays is unknown. The sense of relative movement along the northern segment of the main fault is predominantly normal with a total vertical displacement of 3–3.5 km (LaPoint, 1971; Witkind, 1975; Haller, 1995). Data from a gravity survey has been interpreted to suggest that an estimated total crustal extension of 2 km characterizes this region through a series of horsts and grabens (LaPoint, 1971). However, except for the main Mission Fault, we did not observe surface scarps associated with any of the faults proposed by LaPoint (1971), either onshore or offshore. S_{mf} for the northern segment of the Mission Fault is approximately 1.6 and SL indices range from 218 to 338 (mean = 274).

North of Flathead Lake, the Mission Fault continues onshore as the two easternmost splays of several faults (Mission Fault, Kalispell–Finley Point Fault, Swan Fault) that offset bedrock (Fig. 3A; Stickney, 1980). These generally north–south striking faults define a structural graben that Stickney (1980) termed the Flathead Graben. Stickney (1980) also recognized several NE–SW-trending faults (e.g. Carson Fault), based on recent micro-earthquake activity further to the north, that appear to truncate many of the north–south-trending faults (Fig. 3A). The NE–SW-trending Carson Fault has an oblique-slip sense of motion with normal displacement of the hanging wall to the NW and left-lateral strike-slip. Further north and east, extension is accommodated by the Swan Fault, a major down-to-the-west normal fault en échelon to the Mission Fault (Fig. 3A).

Major bedrock faults west of Big Arm Bay are compiled from gravity survey data (LaPoint, 1971) and surface mapping (Fig. 3A; LaPoint, 1971; Harrison et al., 1986; Hendrix et al., 2004). LaPoint (1971) suggested that the main east–west-trending faults dip vertically and have exclusively strike-slip movement. The Big Draw Fault appears to continue from west of the lake into Flathead Lake and onto Wild Horse Island (Fig. 3A). West of the lake the fault is a right-lateral strike-slip fault. Our mapping on Wild Horse Island suggests also a significant component of right-lateral strike-slip movement for this fault, but some of the movement is accommodated by a normal sense of motion down to the NW (Fig. 3A).

Our observations of strike changes across the onshore trace of the Chief Cliff Fault, north of Big Arm Bay, suggest that it is characterized by left-lateral strike-slip motion (Fig. 3A). In contrast, other major faults north of Big Arm Bay, the Table Bay Fault and Rollins Fault have exclusively normal sense of motion. Results by Harrison et al. (1986) and more recent work by Hendrix et al. (2004) suggest that neither of these faults offset Pleistocene and Holocene sediments onshore.

3.1.2. Faults offshore with predominantly normal sense of movement

Faults with predominantly normal sense of motion are the most common fault type in Flathead Lake, but are confined to the main basin east of Wild Horse Island (Figs. 3A and 4). Normal faults in the lake basin generally displace the hanging wall either to the west or to the east. Total fault separation of reflectors is of very different magnitude across the lake basin and ranges from decimeter scale offset, just within seismic resolution, to fault scarps as high as 14 m.

One of the best-imaged sublacustrine faults with a well-developed scarp is the Mission Fault and, in particular, fault splays B1 and B2 (Figs. 3A, 4A and 5). Fault splay B1 is approximately 15 km long and connects to a 5.8-km-long onshore segment of the Mission Fault north of the lake that was first recognized in a gravity survey by Stickney (1980). All segments have a predominantly normal slip separation of seismic reflections with sense of throw down to the west. Fault splay B2 is another branch of the Mission Fault located about 4.7 km south of Woods Bay (Fig. 1C). Splays B1 and B2 are characterized by steep surface scarps that range between ∼3 m (Fig. 5A and D—lines 35J, 35F) and > 10 m in height (Fig. 5A and D—lines 35G, 35K, 47). Reflections of unit D and younger onlap the steep fault scarps but do not appear to be deformed and thus post-date the offset event (Fig. 5E). However, reflections of unit C are usually chaotic in character (Fig. 5E), rendering determination of offset timing or rate difficult.

Another example of a normal fault with well-defined scarps but a different direction of dip, down-to-the-east, is fault segment B4 of the Kalispell–Finely Point Fault (Figs. 3A, 4A and 6).

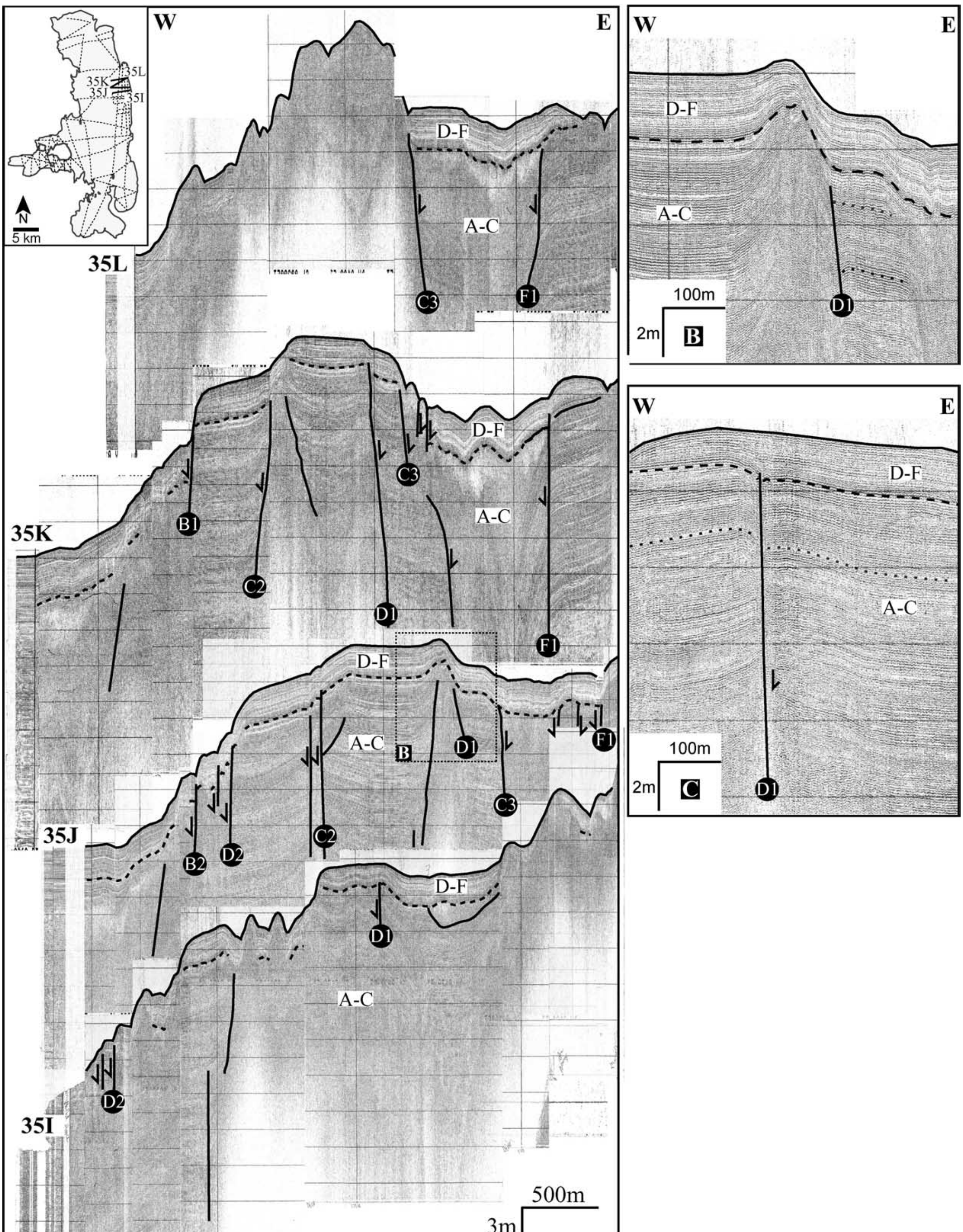

Fig. 5. Display of seismic profiles 35I, 35J, 35K, and 35L (A; see inset map for location) and 35C, 35F, 47, and 35G (D; see inset map for location). Seismic profile 35L is the northernmost and seismic profile 35C the southernmost of these profiles located along strike in the eastern part of the lake. Note the change of fault geometry of several of the faults along strike. The sediment–water interface is marked by solid lines; dashed lines mark the contact between seismic stratigraphic units C and D. Profiles B and C are parts of seismic lines 35J and 47, respectively, showing the detailed geometry of fault D1, an oblique normal fault. The stippled line on this profile is a trace of an example reflector. In profile C the fault dips towards the east, while reflectors displayed in profile B show normal and reverse fault movement—an observation based on drag folding of the reflectors. Displaced reflectors are generally older than seismic unit D. Profile E displays the fault scarp geometry, as common along strike of the Mission Fault. Fault scarps of segments B1 and B2 are between <3 and >10 m high and were formed during tectonic phase B. The steepness of the scarp exceeds the threshold angle for sediment deposition; hence, reflectors of younger units do not drape the fault scarp. Note the high-angle onlap geometry of reflectors in seismic units D–F.

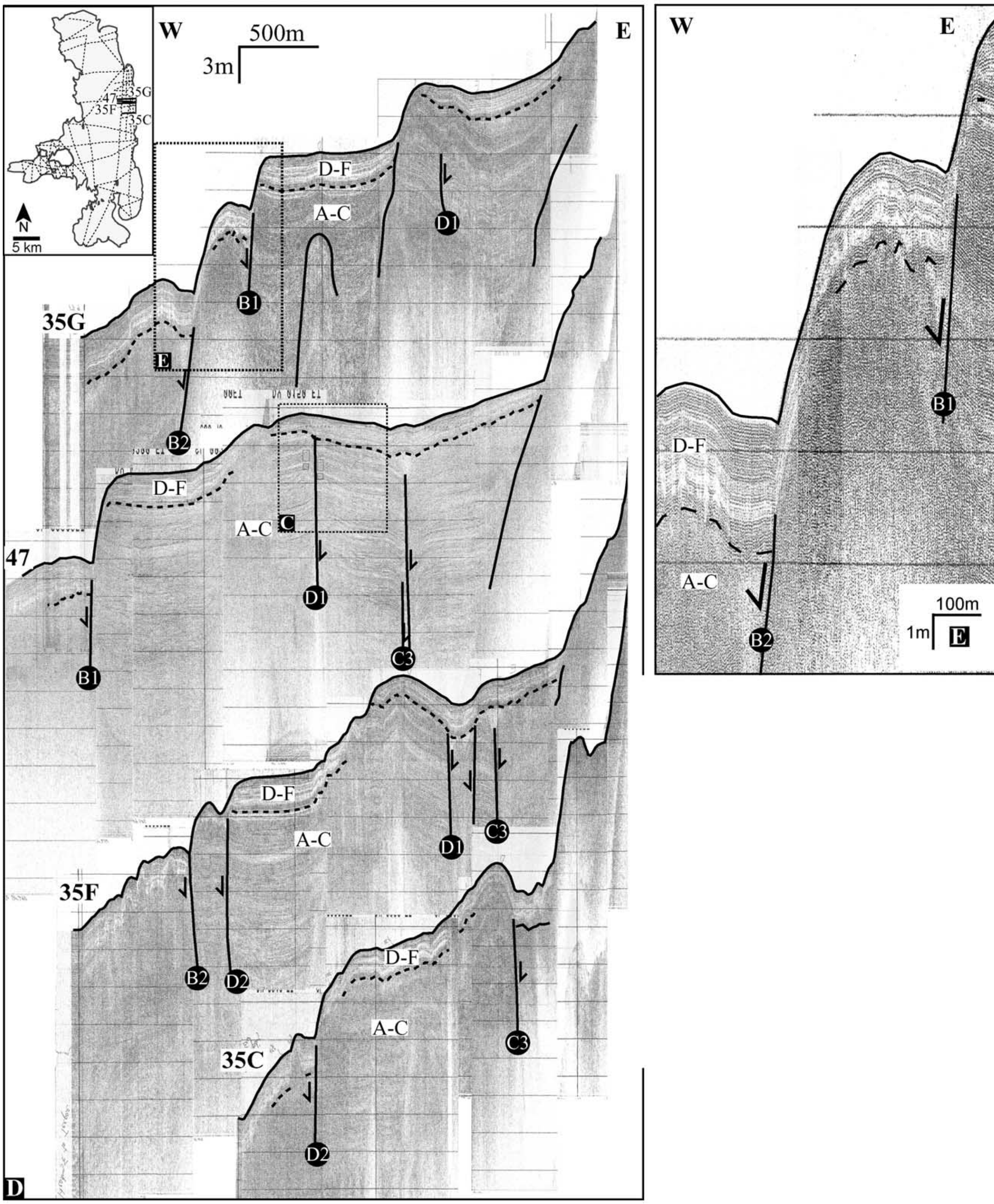

Fig. 5 (*continued*)

Associated with fault splay B4 are steep surface scarps along its southern trace that range between ∼10 and ∼14 m (Fig. 6—lines 24, 6, 17), and decrease in height to the north (Fig. 6—lines 28, 47).

Other normal faults in the lake basin commonly show vertical displacement of reflectors of much smaller scale and no surface expression. Fault splay E1, the offshore segment of the Table Bay Fault, for example, extends for approximately 7 km from 2.2 km east of Cedar Island to the south (Figs. 3A and 4D) and shows normal displacement of reflectors with throw down to the east (Fig. 7). Displacement of lowest unit E and older reflectors corresponds to an approximate age

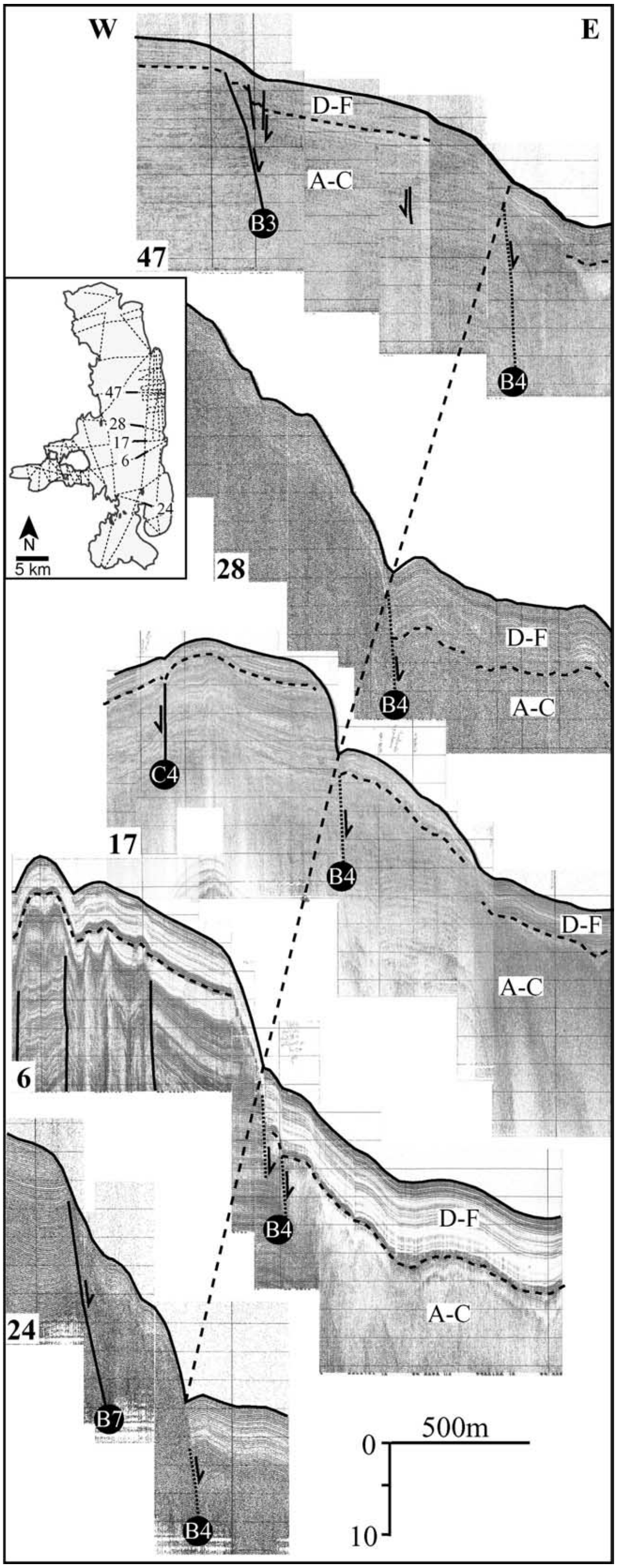

Fig. 6. Composite of several seismic profiles imaging the fault scarps along the Kalispell–Finley Point Fault and in particular fault splay B4. Profile 47 is the northernmost and profile 24 the southernmost seismic profile along strike of this fault (see inset map). Note the decreasing fault scarp height to the north. Movement along this fault occurred most likely during seismic phase B. The dashed line marks the unit C–D contact.

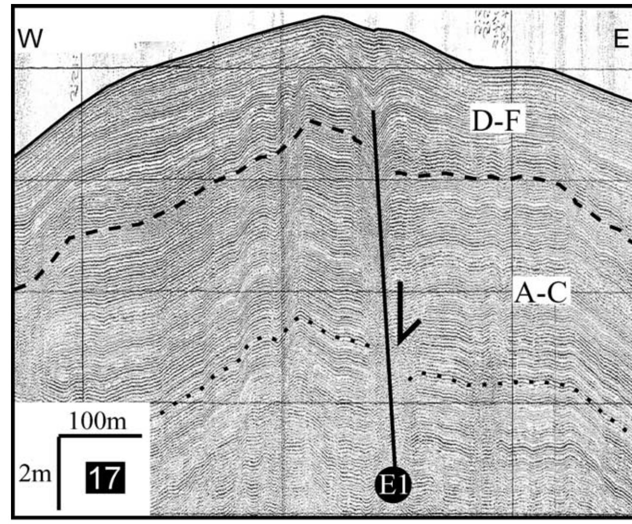

Fig. 7. Part of seismic profile 17, displaying offset along the offshore segment E1 of the Table Bay Fault. Dip of the fault is down to the east and reflectors of unit D are included in the normal fault separation. Stippled line is a trace of an example reflector; the dashed line marks the contact of seismic units C and D.

of 6000–5000 cal yr BP (Hofmann et al., 2006). The offset of unit E and older reflectors ranges between 0.4 and 1.1 m (Fig. 7). Most of the remaining normal faults in the lake basin also have vertical offset of seismic reflections at dm scale, revealing geometries similar to fault splay E1 (Table 1, Fig. 3A).

3.1.3. Normal faults with strike slip movement

The second group of faults recognized in the lake basin includes oblique normal faults and faults with dominantly strike-slip motion. The latter type of faults are imaged as zones of high structural variability, with sense of movement changing along strike between reverse and normal and local variations in the magnitude of throw. This change of structural style along strike is similar to that documented in examples of strike-slip faults mapped onshore (e.g. Christie-Blick and Biddle, 1985), imaged offshore (e.g. Harding, 1983), and synthesized in experimental models (e.g. Richard et al., 1991). Analogous structural geometries also have been described in outcrops of Aptian lacustrine strata from northern Brazil, where Rosetti and Góes (2000) linked similar structures to paleoseismic events and suggested that such a complicated style of deformation might be caused by strike-slip tectonism. A prime example for this type of fault in our data set is the offshore segment (fault splay C6) of the Chief Cliff Fault, located in the western part of the lake (Figs. 3A, 4B and 8). This fault was first recognized by Hofmann et al. (2006) who described this zone of disrupted reflectors (their unit C3) as a zone of liquefaction related to a fault trace. Displacement along this fault occurred just before the deposition of unit D or approximately 10,000 cal yr BP. The downsection termination of many of the smaller faults imaged in this fault zone might be due to the relative orientation of the seismic profile with respect to the dipping

Table 1
Summary of the fault characteristics of all faults in the lake basin. Fault names are the same as in Fig. 3 and fault segment names correlate to fault segments in Fig. 4. For location of faults and fault segments refer to Figs. 3 and 4. Faults correlated to the oldest post-glacial fault activity phase in the lake basin offsets seismic stratigraphic unit B at about 15,000 cal yr BP. Age of displacement and displacement rates correlate well to the oldest late Pleistocene offset along the southern Mission Fault where Ostenaa et al. (1995) suggest a similar age of displacement with comparable displacement rates. Another well constrained tectonic event along the southern Mission Fault at about 7700 cal yr BP also correlates well to fault offset that we observed in the Flathead Lake basin. An event at about 10,000 cal yr BP that we observed in the lake basin is not well constrained from the onshore data set. However, Ostenaa et al. (1995) suggest up to four events that ruptured the southern part of the Mission Valley, including the 15,000 and the 7700 cal yr BP events. Assuming fairly constant recurrence intervals for the study area, a smaller event at about 10,000 cal yr BP might be included in some of the onshore scarps in the southern Mission Valley but of unknown displacement rates. Other phases of tectonic activity after 7700 cal yr BP seem to be more locally confined to the lake basin and do not have any onshore counterpart

Fault name	Segment name	Observed along seismic line	Dip direction	Youngest units offset (age of displacement)	Offset [m] (seismic unit offset), scarp	Displacement rates [mm/yr]	Fault geometry (strike, length, slip)	Southern Mission Fault	
								Activity phases [cal yr BP]	Displacement rate [mm/yr]
MF	B1	18, 20, 21, 30, 35G, 35K, 47	W	B?	*4.3–7.3*	*0.3–0.6*	165–185° southern segment, 170° northern segment, 20 km, normal	~15,000, 12,500–12,600	1.13–1.33, ?
MF	B2	35F, 35G, 35J	W	B?	2.7 (C–D)		176°, 2.9 km, normal		
KFF	B3	21, 47	E						
KFF	B4	6, 17, 23, 24, 28	E	B?	6.1–14.3	0.4–1.1	~350°; 17.5 km, normal		
KFF	B5	28, 30	E	C (13,000–14,000)	1.8–3.3 (upper B)	0.13–0.28	5–358°, 10.9 km, normal		
RF	B6	6, 17	E	lowest C (13,000–14,000)	0.5–0.6 (upper B)	0.03–0.05	355°, 3.2 km		
KFF	B7	24	E	lowest C (13,000–14,000)			3°, 2.3 km long, normal slip		
MF	C1	18	W	C (~10,000)	0.8 (C)	0.19	Normal	10,000–10,300	?
MF	C2	35J, 35K	W	C–D (~10,000)	0.4 (C–D)	0.04	178°, 1.6 km, normal		
MF	C3	35J, 35K, 35L, 35C, 35F, 47	E	C (~10,000)	4.3 (C–D)	0.43	223° southern part, 233° northern part, 2.5 km, normal		
KFF	C4	28	E	C, lowest D (~10,000)			357°, 1.3 km, normal		
MF	C5	6, 23, 27	W	C (~10,000)	1.8 (upper B)	0.13	177–194°, 9.4 km, normal		
CCF	C6	15	S–S	C (~10,000)			Strike–slip		
MF	D1	35I 35F, 35J, 35K, 47	W E	lowest D (~8000)	0.5–0.8 (upper B)	0.03–0.06	352° southern segment, 336° northern segment, 3.8 km, oblique normal		
MF	D2	35C, 35F, 35I, 35J	W	D (~8000)	2.7 (C–D)		155–174°, 4.5 km, normal	7500–7900	0.25–0.4
MF	D3	6, 17	W	D (~7600)	0.7–1.9 (D)	0.09–0.25	194°, 1.9 km, normal		
MF	D4	6	W	D (~7500)	3.3 (D)	0.44	Normal		
TBF	E1	6, 17, 28	E	D, lowest E (5,000–6000)	0.5–1.1 (upper B)	0.09–0.23	340–350°, 7 km, normal		
MF	E2	25	W	lowest E (~5000)	0.4 (D–E)		176°, 5.3 km (2.2 onshore), normal		
MF	F1	35J, 35L, 35K	W	E–F (~1600)	0.7 (C–D)	0.47	155°, 2.5 km, normal		

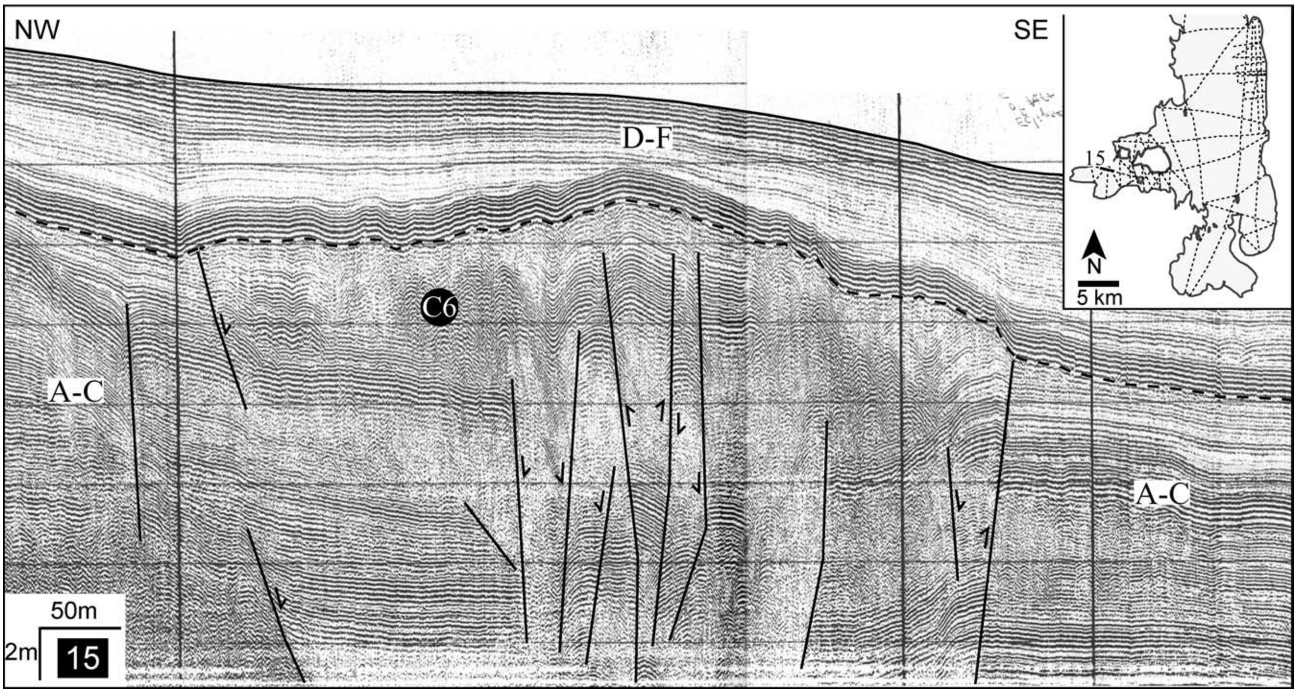

Fig. 8. Strike-slip fault imaged along seismic profile 15. The zone is composed of small-scale faults with normal and reverse sense of motion, typical for strike-slip faults. The direction of movement is unknown, but the onshore segment of this Chief Cliff Fault, north of the lake shows left-lateral movement. This fault is the only major fault in the lake west of Wild Horse Island. The dashed line marks the unit C–D contact (see inset map for location).

fault plane as suggested by Charlet et al. (2005) for faults in Lake Baikal. Oblique normal faults commonly show a considerable variation in structural style similar to strike-slip faults but also have a distinctive normal slip separation of seismic reflectors. The best example of this kind of fault is fault splay D1 of the Mission Fault, a 3.8-km-long splay comprised of several smaller fault segments (Figs. 3A and 4C). The northernmost segment shows predominantly normal slip separation down to the ENE (Fig. 5A—line 35K). Analogous normal slip separation with throw down to the east is also imaged along the southern trace (Fig. 5C and D—lines 47, 35F, 35G). However, the middle segment shows normal fault separation with dip down to the west (Fig. 5A—line 35I) and older strata in line 35J (Fig. 5B) show offset along the same fault splay but with a reverse sense of motion. Together, these observations strongly suggest that fault splay D1 has a significant strike-slip component that in places is the dominant sense of offset. The vertical component of displacement of upper unit B reflectors ranges between 0.5 m for the west dipping fault splay and ~0.8 m for the east dipping fault traces, while vertical offset of younger reflectors (unit C–D) along the northern segment of the fault is ~0.6 m (Fig. 5A—line 35K).

3.2. Neotectonic evolution of the southern Flathead Valley, the Mission Valley, and the Flathead Lake Basin

Most of the faults in the study area have normal sense of motion and strike approximately north–south, in agreement with the overall tectonic stress field of the region that shows the maximum compressive stress orientation ($\sigma 1$) parallel to the main fault's strike direction (Figs. 1A and 3A; Zoback and Zoback, 1989). Faults with some inferred strike-slip sense of motion, in contrast, are generally not oriented parallel to this stress field, hence compensate the compressive component of the stress field by oblique dip-slip or exclusive strike-slip movement (Fig. 3A).

Available data suggest that the structural style of the Mission Fault system varies significantly throughout the length of the southern Flathead and Mission Valleys. The southern part of the Mission Valley seems to be bounded by one major trace of the Mission Fault that has been active during the Holocene (Ostenaa et al., 1995). In contrast, our study shows that the Flathead Lake basin is dissected by numerous faults (Fig. 3). Generally diffuse earthquake activity in the Flathead Valley (Stickney et al., 2000) suggests that the structural style of multiple fault splays and widespread deformation continues north of the lake until these faults are truncated by east–west striking faults (Fig. 3A; Stickney, 1980; Rotstein et al., 2004). However, it is important to mention that a lack of data in the southern part of Flathead Lake and south of the lake might skew the above interpretation.

3.2.1. Phases of tectonic activity

A general picture from our fault interpretation is one of episodic tectonic activity throughout the late Pleistocene and Holocene. Five phases of significant fault displacement were recognized in the lake basin (Table 1), each having very different displacement rates and each being centered about a different location (Fig. 4). The five tectonic phases are named after the youngest reflectors that are cut by a fault. Most of the displacement appears to have occurred in the following phases: (B) 15,000–13,000 cal yr BP, (C) ~10,000 cal yr BP, (D) 8000–7600 cal yr BP, (E) 7500–5000 cal yr BP, and (F) within the last 2000 years. South of the lake in the Mission Valley, Ostenaa et al. (1995) reported at least two and maybe as many as four tectonic events along traces of the Mission Fault since the last major glaciation (~15,000 cal yr BP; Hofmann et al., 2006), with the last of these major events being dated at ~7700 cal yr BP.

Faults included in phase B are all faults in the lake basin that cut seismic reflections of seismic stratigraphic unit B and older. The active fault splays during this oldest tectonic phase generally mimic the main fault trace of the Mission Fault and the Kalispell–Finley Point Fault (Figs. 3A and 4A). Both of these faults are characterized by mostly high and steep fault scarps that are well imaged on several of the seismic profiles. Similar steep fault scarps have been mapped south of the lake along the onshore trace of the Mission Fault (Hofmann and Hendrix, 2004a). Faulting along the active fault splays B1–B7 in the lake basin occurred sometime after the last glacial maximum and the retreat of the Flathead Lobe of the Cordilleran Ice Sheet, because onshore traces of the Mission Fault south of the lake offset glacial sediments. Based on results from trenching studies Ostenaa et al. (1995) recognized a large surface offset with fault scarps as high as 10 m along the southern Mission Fault. Offset occurred prior to the well-dated 7700 cal yr BP event and after deposition of glacial till related to the last glacial maximum. These authors suggested a depositional age of 19,000–23,000 cal yr BP for this glacial till, but more recent studies show that the last maximum ice extent for the Cordilleran Ice Sheet did not occur before ~15,000 cal yr BP (Clague and James, 2002).

Although we cannot demonstrate an obvious offset/drape relationship of seismic reflections of relevant age in the lake (Figs. 5 and 6), we are still confident with our interpretation of the timing of this oldest event based on the following observations: (A) along the high scarps, parallel seismic reflectors younger than ~15,000–13,000 cal yr BP do not show any signs of obvious drag folding that would indicate more recent movement along these faults. Instead, many of these younger reflections onlap the toe of the fault scarps at a high angle (Fig. 5E). (B) We suggest that this geometry is purely depositional in nature and younger sediments were not draped over many of these scarps because the angle of these scarps exceeds the threshold angle for sediment accumulation. Alternatively, the scarps might be covered by a thin drape of sediment that is well below seismic resolution. (C) Some of these fault scarps occur in parts of the lake where chaotic seismic reflections (seismic unit C2 in Hofmann et al., 2006) are dominant and movement along the particular fault and/or deformation of reflections is not well imaged in the seismic record. However, based on the spatial distribution of the chaotic reflections of seismic stratigraphic unit C2, described as turbidite deposits (Hofmann et al., 2006) we suggest that they were deposited in this structurally controlled trough in the eastern part of the lake. The formation of the steep fault scarps associated with the Kalispell–Finley Point and Mission Faults pre-date the deposition of this seismic stratigraphic unit and were in fact the confining margins for these sediment gravity flows.

Based on all these observations we suggest that the fault scarps along several onshore segments of the Mission Fault and the high scarps along several offshore segments of the Mission and Kalispell–Finley Point Faults (splays B1–B5; Figs. 4A, 5 and 6) were formed during the same seismic event just after the deposition of the glacial till (seismic stratigraphic unit A) between 13,000 and 15,000 cal yr BP. This oldest observed rupture event was the main displacement event in the lake basin during the latest Pleistocene.

Included in the second phase (C) of displacement at the end of the deposition of seismic unit C (~10,000 cal yr BP) are many different splays of several faults in the lake (C1–C6; Fig. 4B). Most fault splays active during phase C strike north–south and are characterized by exclusively normal sense of motion. Only fault splay C6, the offshore segment of the Chief Cliff Fault located in the western part of the lake and also active during this tectonic phase, strikes NW–SE and has notable strike-slip movement (Fig. 8). During phase D, displacement of unit D and older reflections occurred along fault splays in the far eastern part of the lake (Fig. 4C), close to the main trace of the Mission Fault. Phase D is coeval with the last major fault offset reported from the southern segment of the Mission Fault (Table 1; Ostenaa et al., 1995), although offset in the lake was of smaller scale. In contrast, ruptures during the two youngest phases (E and F) that post-date the deposition of the Mount Mazama tephra (7630±80 cal yr BP) appear to be restricted to just three fault splays and could not be linked to any other rupture events in the Mission or Flathead Valleys (Fig. 4D, Table 1).

3.2.2. Displacement rates

To evaluate total vertical fault displacement rates for the lake basin, we assigned an equally spaced grid of 10 fields perpendicular to the maximum regional compressive stress field across the lake. Then we calculated the total displacement rates for each of these fields by summing the displacement rates of single fault splays located in the grid (Fig. 9A).

The results of the total displacement in the lake basin are based on the displacement rates that we measured for each of the fault splays (Table 1). Displacement rates for faults of phases C–E are widely spread and range between 0.03 and 0.43 mm/yr but culminate at displacement rates of less than 0.1 mm/yr (Table 1). The timing of movement along the different splays is constrained by known reflectors such as the Mount Mazama tephra (7630±80 cal yr BP) and other seismic stratigraphic units recognized by Hofmann et al. (2006). Most splays of these young faults in the lake basin were only active during one of these late Pleistocene or Holocene displacement events, although parts of fault splay D1 show evidence for displacement during two separate events within the last 15,000 cal yr BP.

Total displacement rates for this young set of faults (phases C–E) range from 0.08 to 0.23 mm/yr (Fig. 9A). We found that the lowest displacement rates occurred in the south and higher

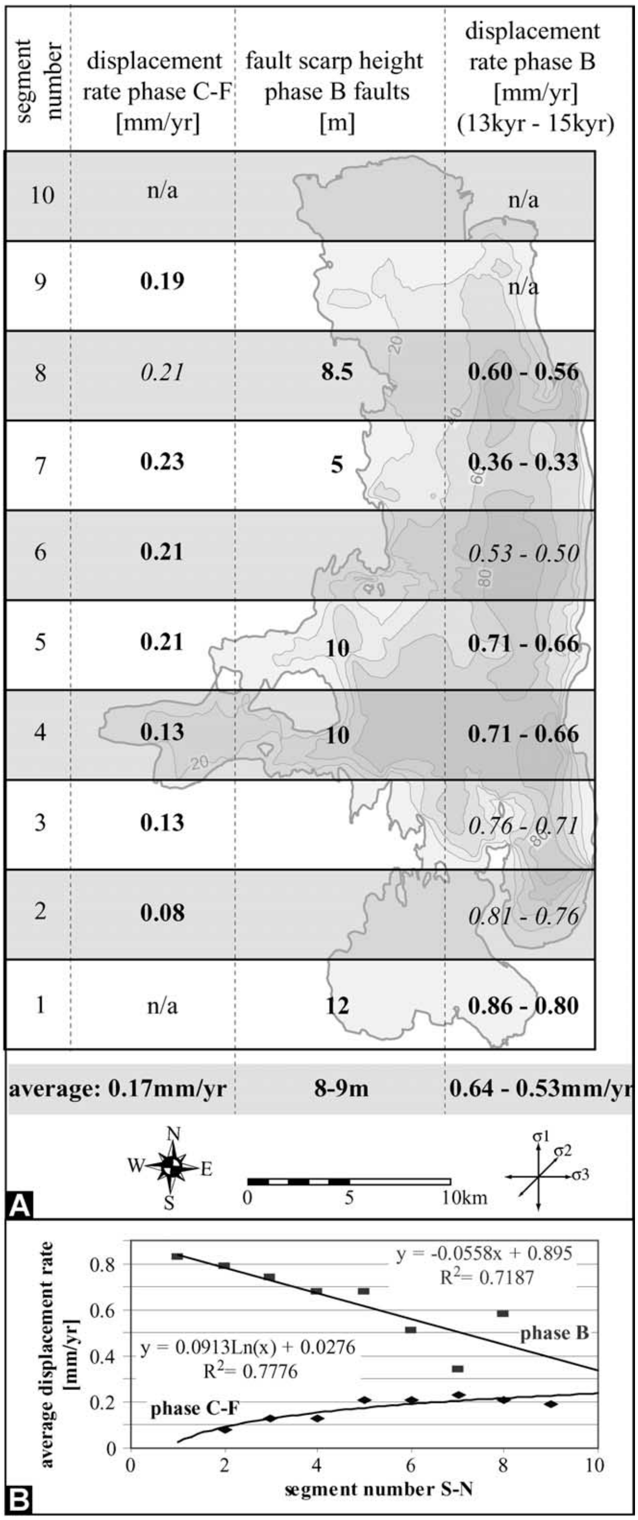

Fig. 9. (A) Average displacement rates in the Flathead Lake basin. Flathead Lake is subdivided into 10 grids, each grid parallel to the main extensional stress vector for the region. Displacement rates for each of the grids are displayed for phases C–F and phase B. Additionally we displayed the average fault scarp height for faults inferred to have been active during phase B. Bold numbers are measured data points, italic numbers are interpolated displacement values. (B) In general, displacement rates and fault scarp heights for phase B decrease to the north following a linear trend with a R^2 of ~ 0.72 and reflecting decreasing fault activity in the same direction. Displacement rates of phases C–F increase slightly towards the center of the lake and start decreasing further to the north. The best-fit trend line is logarithmic with an R^2 of ~ 0.78. However, the displacement rate for the southernmost grid is most likely underestimating the actual displacement due to a lack of data and displacement rates for units C–F are more likely fairly constant throughout the lake basin.

displacement rates in the center and northern part of the lake (Fig. 9B), but this interpretation might be limited because displacement rates in the southern part of the lake are likely to be underestimated due to the lack of seismic reflection data in this area. In general, however, such low displacement rates are similar to average displacement rates calculated for the southern Mission Fault segments and fit well in the range of neotectonic faults reported from other moderate seismically active areas (Wallace, 1984; McCalpin, 2003). These low displacement rates also match well with the relatively short nature of these faults with an average length of less than 2.5 km (Table 1, Figs. 3A and 4). Nicol et al. (1997, 2005) showed that short faults generally have a lower capability for large displacement rates and high frequency recurrence intervals relative to long faults.

In contrast to the short fault segments of the younger faults, fault segments of the main Mission Fault and the Kalispell–Finley Point Fault are longer (B1, B2 and B4; Fig. 3A) and thus are capable of higher displacement rates (Nicol et al., 1997, 2005). As a result, fault scarps related to the last rupture event along these long fault splays (13,000 and 15,000 cal yr BP) range between 3 and 14 m in height (Figs. 5 and 6). Onshore and offshore data suggests that offset along these faults represent likely one rupture event, thus displacement rates range between ~ 0.3 and ~ 0.9 mm/yr (Fig. 9A). Importantly, the displacement rates for phase B decrease linearly to the north within the lake basin, suggesting a lower tectonic activity in the northern part of the lake (Fig. 9B). These displacement rates are consistent with the calculated S_{mf} and SL indices for the northern Mission Fault segment that also suggest a high to moderate tectonic activity class of 2 to 3 (e.g. Keller and Pinter, 1996). We also calculated displacement rates for the southern Mission Fault segment where Ostenaa et al. (1995) described up to 12-m-high fault scarps in glacial till. Based on trenching studies by these authors, a younger tectonic event (7700 cal yr BP) is responsible for a surface offset of 2–3 m. We suggest that 9–10 m of the displacement is likely related to the older event that occurred between 13,000 and 15,000 cal yr BP resulting in an average displacement rate ranging from 1.23–1.43 mm/yr for the latest Pleistocene and early Holocene to 0.26–0.39 mm/yr since the last seismic event at 7700 cal yr BP. Displacement rates for this fault segment are slightly higher than in the northern part of the study area but correlate well to the low value of S_{mf} and the high SL-indices that we calculated for this fault segment and are typical for faults of a high tectonic activity class (Rockwell et al., 1985).

In general the average displacement rates in the lake basin for the last 10,000 cal yr BP (phases C–F) are relatively low (Table 1, Fig. 9), implying a recent low in tectonic activity in the study area. Most of the displacement was probably from low magnitude earthquakes, as they occur frequently in the study area (Stickney et al., 2000). In contrast the average displacement rates calculated from the oldest event (phase B) are significantly higher (Table 1, Fig. 9). We suggest that these higher rates are probably closer to the long-term displacement rates of the valley because of the low S_{mf} values, high SL values, and the resulting high tectonic activity classes for parts of the Mission Fault.

The high relief fault scarps mapped along the main trace of the Mission Fault system may be related to one or more large magnitude earthquakes. For example, in Bear Lake Valley, Utah, McCalpin (2003) linked ~6-m-high fault scarps in late Pleistocene sediments to earthquake magnitudes of ~7.2, and 6 m fault scarps in the vicinity of Hebgen Lake, Montana are related to the magnitude 7.5 historic Hebgen Lake earthquake (Stickney et al., 2000). Based on these data, a total displacement of up to 14 m as measured along some of the fault splays in the study area likely requires an earthquake of magnitude >7.5. Given the low Holocene displacement rates, the region currently is in a seismically quiescent phase. It seems just a matter of time before another large magnitude earthquake will bring the overall displacement rates back to average.

4. Conclusion

1. Integrated analysis of 3.5 kHz seismic reflection profiles, onshore geologic mapping, and review of relevant literature indicates that the Mission Fault system of western Montana changes character significantly along strike, from a single strand along its southern length to multiple strands further to the north within the Flathead Lake basin. The Mission Fault system is dominated by normal-slip faults oriented perpendicular to the regional extensional stress direction but also contains a subordinate set of oblique-slip and strike-slip faults that strike at a shallower angle to the regional extensional stress direction.
2. Analysis of stratal cross-cutting relations within the seismic data set from Flathead Lake reveals the presence of five different phases of increased seismic activity occurring at 15,000–13,000, ~10,000, 7900–7600, ~7500–5000, and within the past 2000 cal yr BP. The phases that occurred at 15,000–13,000 and 7900–7600 years correlate best with fault scarp analysis studies conducted along the southern strand of the Mission Fault located onshore about 30 km south of Flathead Lake.
3. Displacement rates calculated for the oldest phase of tectonic activity and for the combined four younger phases of tectonic activity suggest that displacement rates decrease to the north for the older phase of activity and increase slightly to the north across the lake basin for the younger phases. A substantial decrease in displacement rate characterizes the transition from the earliest phase to the younger combined phases, suggesting that a major seismic event is due to return the displacement rate back to its longer term average.

Acknowledgements

We are grateful to the Confederated Salish and Kootenai tribes for permission to conduct this study on tribal lands. Comments from Jim Sears, Chuck Kluth, and Larry Smith greatly improved earlier versions of this manuscript and are highly appreciated. We also thank Amy Bondurant, Ed Salmon, and Donovan Power for assistance in the field. Hofmann would like to acknowledge the United States Geological Survey EDMAP program, the Geological Society of America, the American Association of Petroleum Geologists, and The University of Montana for research grants to accomplish this study. Hendrix and Moore thank the National Science Foundation (grant # ATM-0214273) for supporting this work.

References

Alden, W.C., 1953. Physiography and glacial geology of western Montana and adjacent areas. U.S. Geological Survey Professional Paper 231.

Bull, W.B., 1987. Relative rates of long-term uplift of mountain fronts. U.S. Geological Survey Open File Report 87-673, pp. 192–202.

Charlet, F., Fagel, N., De Batist, M., Hauregard, F., Minnebo, B., Meischner, D., SONIC Team, 2005. Sedimentary dynamics on isolated highs in Lake Baikal: evidence from detailed high-resolution geophysical data and sediment cores. Global and Planetary Change 46, 125–144.

Christie-Blick, N., Biddle, K.T., 1985. Deformation and basin formation along strike-slip faults. Society of Economic Paleontologists and Mineralogists Special Publication 37, 1–34.

Clague, J.J., James, T.S., 2002. History and isostatic effects of the last ice sheet in southern British Columbia. Quaternary Science Reviews 21, 71–87.

Constenius, K., 1996. Late Paleogene extensional collapse of the Cordilleran foreland fold and thrust belt. Geological Society of America Bulletin 108, 20–39.

Davis, W.M., 1920. Features of glacial origin in Montana and Idaho. Annals of the Association of American Geographers, 75–148.

Finckh, P., Kelts, K., Lambert, A., 1984. Seismic stratigraphy and bedrock forms in perialpine lakes. Geological Society of America Bulletin 95, 1118–1128.

Haller, K.M., 1995. Fault number 699, Mission Fault, Flathead Lake section. In: Quaternary Fault and Fold Database of the United States, ver.1.0, U.S. Geological Survey Open-File Report 03-417.

Haller, K.M., Tsutsumi, H., Machette, M.N., Essex, J., Hancock, D., 2000. Paleoseismology of the Grayling Creek site, red Canyon fault (1959 Hebgen Lake, Montana, Earthquake). Eos Transactions AGU 81, 1169.

Harding, T.P., 1983. Divergent wrench fault and negative flower structure, Andaman Sea. American Association of Petroleum Geologists Studies in Geology Series 15-3, 4.2.1–4.2.11.

Harrison, J.E., Cressman, E.R., Whiple, J.W., 1986. Geologic and structure maps of the Kalispell 1°×2° quadrangle, Montana, and Alberta and British Columbia. USGS Miscellaneous Investigations Series Map I-2267, scale 1:250,000.

Hendrix, M.S., Bondurant, A.K., Timmerman, G., Salmon, E.L. III, 2004. Preliminary results from geologic mapping and sedimentologic analysis of late Pleistocene glacial and post-glacial deposits, southern Flathead and northern Mission Valleys, western Montana. Geological Society of America, Abstracts with Programs 36.

Hofmann, M.H., Hendrix, M.S., 2004a. Geologic map of the East Bay 7.5′ Quadrangle, Northwest Montana. Montana Bureau of Mines and Geology, Open-File Report 496, scale 1:24,000.

Hofmann, M.H., Hendrix, M.S., 2004b. Geologic map of parts of the Arlee, St. Ignatius, Gold Creek, and St. Mary's Lake 7.5′ Quadrangles, Northwest Montana. Montana Bureau of Mines and Geology, Open-File Report 497, scale 1:24,000.

Hofmann, M.H., Hendrix, M.S., Moore, J.N., Sperazza, M., 2006. Late Pleistocene and Holocene depositional history of sediments in Flathead Lake, Montana: evidence from high-resolution seismic reflection interpretation. Sedimentary Geology 184, 111–131.

Keller, E.A., Pinter, N., 1996. Active Tectonics—Earthquakes, Uplift, and Landscape. Prentice Hall, New Jersey.

Kogan, J., 1980. A seismic sub-bottom profiling study of recent sedimentation in Flathead Lake, Montana. MSc thesis, University of Montana.

Lageson, D.R., Stickney, M.C., 2000. Seismotectonics of Northwest Montana, USA. In: Schalla, R.A., Johnson, E.H. (Eds.), Montana Geological Society 50th Anniversary Symposium, Montana/Alberta Thrust Belt and Adjacent Foreland, pp. 109–126.

LaPoint, D.J., 1971. Geology and geophysics of the southwestern Flathead Lake Region, Montana. MSc thesis, University of Montana.

Leech, G.B., 1966. The Rocky Mountain trench. Canada Geological Survey Paper 66-14, pp. 307–329.

Levish, D.R., 1997. Late Pleistocene sedimentation in glacial Lake Missoula and revised glacial history of the Flathead lobe of the Cordilleran ice sheet, Mission Valley, Montana. Ph.D. thesis, University of Colorado.

McCalpin, J.P., 2003. Neotectonics of Bear Lake Valley, Utah and Idaho; a preliminary assessment. Utah Geological Survey Miscellaneous Publication 03-4.

Miall, A.D., 2000. Principles of Sedimentary Basin Analysis. Springer, Berlin.

Mullins, H.T., Hinchey, E.J., Wellner, R.W., Stephens, D.B., Anderson, W.T., Dwyer, T.R., Hine, A.C., 1996. Seismic stratigraphy of the Finger Lakes: a continental record of Heinrich event H-1 and Laurentide Ice Sheet instability. In: Mullins, H.T., Eyles, N. (Eds.), Subsurface Geologic Investigations of New York Finger Lakes: Implications for Late Quaternary Deglaciation and Environmental Change Geological Society of America Special Paper 311, pp. 1–35.

Nicol, A., Walsh, J.J., Watterson, J., Underhill, J.R., 1997. Displacement rates of normal faults. Nature 390, 157–159.

Nicol, A., Walsh, J.J., Manzocchi, T., Morewood, N., 2005. Displacement rates and average earthquake recurrence intervals on normal faults. Journal of Structural Geology 27, 541–551.

Nobles, L.H., 1952. Glacial geology of the Mission Valley, western Montana. Ph.D. thesis, Harvard University.

O'Neill, J.M., Lonn, J.D., Lageson, D.R., Kunk, M.J., 2004. Early Tertiary Anaconda metamorphic core complex, southwestern Montana. Canadian Journal of Earth Sciences 41, 63–72.

Ostenaa, D.A., Manley, W., Gilbert, J., LaForge, R., Wood, C., Weisenberg, C.W., 1990. Flathead Reservation regional seismotectonic study: an evaluation for Dam safety. U.S. Bureau of Reclamation, Seismotectonic Report 90-8.

Ostenaa, D.A., Levish, D.R., Klinger, R.E., 1995. Mission fault study. U.S. Bureau of Reclamation Seismotectonic Report 94-8.

Pardee, J.T., 1910. The glacial Lake Missoula. Journal of Geology 18, 376–386.

Pardee, J.T., 1942. Unusual currents in glacial Lake Missoula. Geological Society of America Bulletin 53, 569–1600.

Pierce, K.L., Lageson, D.R., Ruleman, C.A., Hintz, R.G., 2000. Holocene paleoseismology of Hebgen normal fault, MT: the Cabin Creek site of the Hebgen Lake Paleoseismology Working Group. Eos Transactions AGU 81, 1170.

Qamar, A.I., Kogan, J., Stickney, M.C., 1982. Tectonics and recent seismisity near Flathead Lake, Montana. Bulletin of the Seismological Society of America 71, 1591–1599.

Richard, P.A., Mocquet, B., Cobbold, P.R., 1991. Experiments on simultaneous faulting and folding above a basement wrench fault. Tectonophysics 188, 133–141.

Rockwell, T.K., Keller, E.A., Johnson, D.L., 1985. Tectonic geomorphology of alluvial fans and mountain fronts near Ventura, California. In: Morisawa, M., Hack, J.T. (Eds.), Tectonic Geomorphology Binghampton Symposia in Geomorphology, International Series 15, pp. 183–207.

Rosetti, D.F., Góes, A.M., 2000. Deciphering the sedimentological imprint of paleoseismic events: an example from the Aptian Codó Formation, northern Brazil. Sedimentary Geology 135, 137–156.

Rotstein, Y., Shaliv, G., Rybakov, M., 2004. Active tectonics of the Yizre'el valley, Israel, using high-resolution seismic reflection data. Tectonophysics 382, 31–50.

Schwartz, D.P., Hebgen Lake Paleoseismology Working Group, 2000. Recurrence of large earthquakes along the 1959 surface rupture at Hebgen Lake, Montana. Eos Transactions AGU 81, 1160.

Sears, J.W., 2001. Emplacement and denudation history of the Lewis–Eldorado–Hoadley thrust slab in the Northern Montana Cordillera, USA: implications for steady-state orogenic processes. American Journal of Science 301, 359–373.

Sears, J.W., Hendrix, M.S., 2004. Lewis and Clark line and the rotational origin of the Alberta and Helena Salients, North American Cordillera. Geological Society of America Special Paper 383, 173–186.

Smith, D.G., 1977. Glacial geology of the Big Arm region of Flathead Lake. In: Glacial Geology of Flathead Valley and Catastrophic Drainage of Glacial Lake Missoula. GSA Rocky Mountain Section, Field Guide 4, pp. 1–13.

Smith, L.N., 2004. Late Pleistocene stratigraphy and implications for deglaciation and subglacial processes of the Flathead lobe of the Cordilleran Ice Sheet, Flathead Valley, Montana, USA. Sedimentary Geology 165, 295–332.

Smith, R.B., Sbar, M.L., 1974. Contemporary tectonics and seismicity of the western United States with emphasis on the Intermountain seismic belt. Geological Society of America Bulletin 85, 1205–1218.

Stickney, M.C., 1980. Seismicity and gravity studies of faulting in the Kalispell Valley, Northwest Montana. MSc thesis, University of Montana.

Stickney, M.C., 1999. Characteristics of recent seismicity in southwest Montana and its relation to late Quaternary faults. Seismological Research Letters 70, 237.

Stickney, M.C., Bartholomew, M.J., 1987. Seismicity and late Quaternary faulting of the Basin and Range Province, Montana and Idaho. Bulletin of the Seismological Society of America 77, 1602–1625.

Stickney, M.C., Haller, K.M., Machette, M.N., 2000. Quaternary faults and seismicity in western Montana. Montana Bureau of Mines and Geology Special Publication 114.

Wallace, R., 1984. Patterns and timing of late Quaternary faulting in the Great Basin province and relation to some regional tectonic features. Journal of Geophysical Research 89, 5763–5769.

Witkind, I.J., 1975. Preliminary map showing known and suspected active faults in western Montana. U.S. Geological Survey Open-File Report 75-285, pp. 1–36.

Wold, R.J., 1982. Seismic reflection study of Flathead Lake, Montana. U.S. Geological Survey, miscellaneous field studies, map MF-1433, scale 1:117,647.

Zoback, M.L., Zoback, M.D., 1989. Tectonic stress field of the continental United States. Geological Society of America Memoir 172, 523–539.